Bioorganic & Medicinal Chemistry Letters 20 (2010) 2765–2769

Contents lists available at ScienceDirect

Bioorganic & Medicinal Chemistry Letters

journal homepage: www.elsevier.com/locate/bmcl

Synthesis and biological activity of 2*H*-quinolizin-2-one based p38α MAP kinase inhibitors

Robert M. Tynebor [a,*], Meng-Hsin Chen [a], Swaminathan R. Natarajan [a], Edward A. O'Neill [b], James E. Thompson [b], Catherine E. Fitzgerald [b], Stephen J. O'Keefe [b], James B. Doherty [a]

[a] Department of Medicinal Chemistry, Merck Research Laboratories, PO Box 2000, Rahway, NJ 07065, USA
[b] Department of Inflammation Research, Merck Research Laboratories, PO Box 2000, Rahway, NJ 07065, USA

ARTICLE INFO

Article history:
Received 8 February 2010
Revised 16 March 2010
Accepted 17 March 2010
Available online 21 March 2010

Keywords:
p38α inhibitors
MAP kinase

ABSTRACT

The development and synthesis of potent p38α MAP kinase inhibitors containing a 2*H*-quinolizin-2-one platform is described. Evolution of the 2*H*-quinolizin-2-one series from an early lead to solving off target activity and pharmacokinetic issues is also discussed.

Over the last decade the pharmaceutical industry invested significant resources in developing a therapy to regulate tumor necrosis factor (TNF-α) for the treatment of such indications as rheumatoid arthritis, psoriatic arthritis, and inflammatory bowel disease.[1] Current TNF-α treatments include monoclonal antibodies Infliximab (Remicade®), Adalimumab (Humira®), and the fusion protein Etanercept (Enbrel®).[2] Although current therapies successfully reduce TNF-α levels, long term patient compliance is compromised by safety, cost, and/or efficacy.[1,3] Currently no small molecule therapy has successfully reached the market.[2]

It has been demonstrated that inhibiting p38α mitogen-activated protein (MAP) kinase delays the onset of joint disease in animal models of arthritis by arresting the over production of pro-inflammatory cytokines such as TNF-α.[4] In peripheral mononuclear blood cells, the p38 MAP kinase pathway is activated by a variety of external stress stimuli, such as heat shock, osmotic stress, lipopolysaccharide (LPS) and other cytokines.[5] Cell surface receptors recognize these stress stimuli and initiate a signal transduction cascade that proceeds through p38 MAP kinase. The upstream activators of p38 MAP kinase are MKK3 and MKK6 while the downstream substrates include MAPKAP kinase-2 and heat shock protein (HSP)-27. The end result is the production of pro-inflammatory cytokines, edema, and joint destruction. Inhibiting of the p38α pathway is therefore expected to down regulate TNF-α production and afford an opportunity to slow the progression of TNF-α mediated inflammatory diseases. In our laboratory we have investigated a new structural class of potent and selective p38 inhibitors utilizing a 6-(2,4-difluorophenyl)-1-phenyl-2*H*-quinolizin-2-one (Fig. 1) scaffold as a pharmacophore, which is the subject of this communication.

Small molecule p38α inhibitors made a structural transition from the tetrasubstituted imidazole series (**2**)[6] to pyrimido pyridazinone derived compounds with the discovery of VX-745 **(3)** (Fig. 2).[7] Investigations into the binding mode of **3** revealed several unique features including a novel induced fit by causing a rotation or 'flip' of the peptide bond between Met-109 and Gly-110. As shown in Figure 2, the tetrasubstituted imidazoles bind to the p38α active site by utilizing a pyrimidine nitrogen to hydrogen bond with Met-109 while **3** binds to the p38α active site by using a carbonyl group to hydrogen bond with Met-109. The second available lone pair on the carbonyl oxygen induces a unique 'flip' of the peptide between Met-109 and Gly-110. The newly reorganized enzyme conformation is then stabilized by the uniquely polar scaffold of **3**.[8,9] MAP kinases outside the p38α,β,γ isoform family fail to adopt the 'flipped' conformation due to larger side chains present at the amino acid residue 110 that make proper enzyme rotation energetically unfavorable. As a result, **3** possessed unprecedented selectivity over a broad range of kinases as well as other closely related members of the MAP kinases family.[9]

It was also hypothesized that the piperidine of **2** interacts with Asp-168 via a water bridged hydrogen bonding interaction. This hypothesis helped drive binding and functional potency in the quinazolinone (**4**) series by utilizing a piperazine to interact with Asp-168. Although functional activity and physical properties were enhanced by the basic amine, such inhibitors were plagued

* Corresponding author. Tel.: +1 215 652 3636; fax: +1 215 652 3971.
E-mail address: Robert_tynebor@merck.com (R.M. Tynebor).

0960-894X/$ - see front matter © 2010 Elsevier Ltd. All rights reserved.
doi:10.1016/j.bmcl.2010.03.069

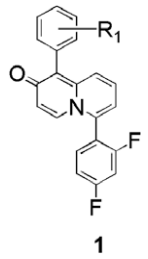

1

Figure 1. 6-(2,4-Difluorophenyl)-1-phenyl-2*H*-quinolizin-2-one.

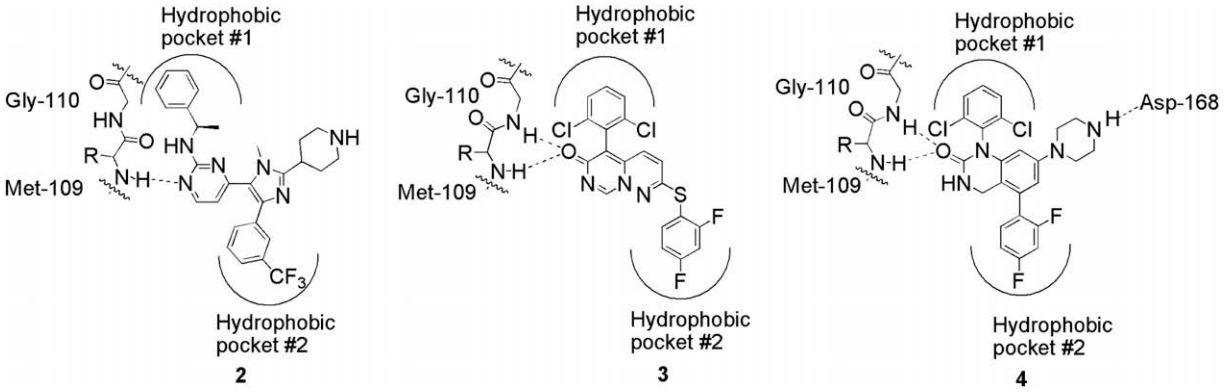

Figure 2. p38α binding schematic for tetrasubstituted imidazole **2**, **3**, and quinazolinone **4**.

with potent ion channel activity. Evolution of small molecule p38α inhibitors focused on replacing the piperazine group of **4**.

Previous research revealed the entire piperazine substituent could be replaced with a simple amino group without a significant loss in functional potency.[10] However this required that the core template had sufficient polarity to achieve good cell potency. Replacing the urea derived core of **4** with a naphthyridinone and the piperazine with an amino group lowered log *D* for compound **5** while maintaining good activity in the LPS stimulated THP-1 cells and human whole blood (hWB) TNF-α release functional assays. Encouraged by the success of **5** we hypothesized that the isomeric quinolizin-2-one **6** derivative would sufficiently increase the core polarity and dipole moment to excise the amine of **5**. In the event, quinolizin-2-one **6** increased scaffold polarity as indicated by the lower log *D* value in Table 1, producing biological activity comparable to compounds **4** and **5**.

Removing the basic amine from compounds **4** and **5** successfully reduced MK-499 activity of quinolizin-2-one **6** to less than 20 μM, but unfortunately other liabilities such as pregnane X receptor (PXR) activation (EC_{50} 3.3 μM) and a long half life in dog (20 h) and monkey (>100 h) precluded further development of **6**. Previous research indicated chemically diverse substituted A-rings were well tolerated.[15] Therefore, we sought to introduce chemically diversity to the A-ring position in an attempt to reduce PXR activation and improve pharmacokinetic properties.

The first series of A-ring modified quinolizin-2-one derivatives focused on the 2,4,6 substitution pattern. Synthesis of such derivatives began with preparation of benzyl bromide **8** via a reaction of the mesylate derived from **7** with LiBr (Scheme 1). Treatment of bromide **8** with activated zinc generated the zinc bromide derivative in situ which was coupled with 2,6 dibromopyridine to yield diaryl methylene **9**. Suzuki coupling between pyridyl bromide **9**

Table 1
Evolution of p38α inhibitors

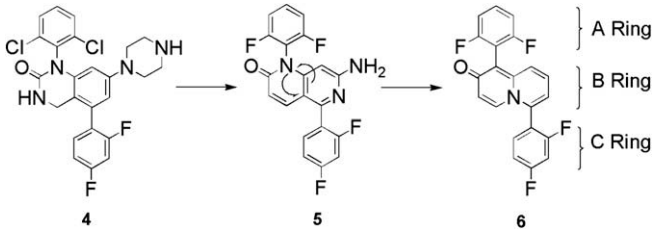

4 5 6

	p38α[6,11] IC_{50} (nM)	THP-l/TNF-α[12] IC_{50} (nM)	hWB/TNF-α[6] IC_{50} (nM)	Log *D*	Ca^{2+} IC_{50}[a] (μM)	*i*Kr[b] K_i (μM)
4	2.6	4.0	76	4.2	0.94	0.87
5	0.6	1.0	34.3	2.7	4.6	5.1
6	7.1	5.6	75.5	2.5	>30	>20

[a] Inhibition of diltiazem binding.[13]
[b] Inhibition of MK-499 binding to hERG in HEK293 cells.[14]

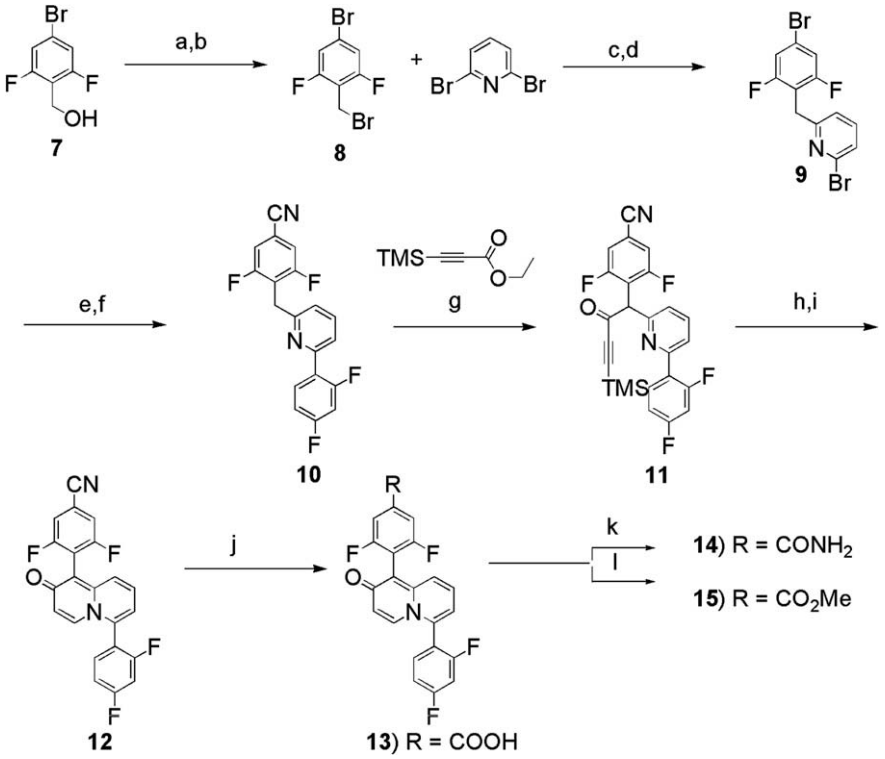

Scheme 1. Synthesis of 2,4,6 substituted A-ring 2*H*-quinolizin-2-one derivatives. Reagents and conditions: (a) MsCl, TEA, CH_2Cl_2, 0 °C warm to rt; (b) LiBr, DMF, 90 °C 45 min, 75% two steps; (c) Zn, THF, 0 °C warm to rt, 1 h; (d) $Pd(PPh_3)_4$ 90 °C, 1 h, 68% two steps; (e) 2,4 difluoro phenyl boronic acid, $Pd(PPh_3)_4$, toluene/EtOH/2 M Na_2CO_3 (10:1:1), 89%; (f) $Zn(CN)_2$, tris(dibenzylideneacetone)dipalladium, 1,1′-bis(diphenylphosphino)ferrocene, DMF/H_2O (100:1), 120 °C, 1 h, 96%; (g) LiHMDS, −78 °C, 1 h, THF, 84%; (h) TBAF, THF, 0 °C, 89%; (i) NMP, 90 °C, 38%; (j) 2 N KOH, dioxane, 90 °C, 24 h, 83%; (k) EDC, hobt, NH_4OH, NMP, 75%; (l) oxalyl chloride, MeOH, 0 °C, 90%.

Table 2
Biological activity of 2,4,6 substituted A-ring 2*H*-quinolizin-2-one derivatives

	p38α IC_{50} (nM)	THP-l/TNF-α[12] IC_{50} (nM)	hWB/TNF-α[6] IC_{50} (nM)	PXR EC_{50} (μM)
12	1.5	6490	N/A	>30
14	20	180	980	>30
15	1.5	6490	N/A	>30

and 2,4 difluoro phenyl boronic acid was used to introduce the C-ring. The nitrile of **10** was installed via a $Pd_2(dba)_3$, dppf, and zinc cyanide coupling with the A-ring bromide. LiHMDS generated the benzylic anion of **10** and was quenched with TMS propenyl ethyl ester to yield the protected diarylbutynone **11**. Removal of the TMS protecting group and thermal cyclization generated the 2*H*-quinolizin-2-one platform **12**.[16]

Nitrile **12** not only served as a valuable synthetic intermediate for future manipulations but also eliminated the PXR activation associated with compound **6** (Table 2). Although the nitrile possessed only weak functional activity, this discovery encouraged the exploration of other heteroatom containing functional groups at this position. Hydrolysis of nitrile **12** to carboxylic acid **13** and EDC coupling with ammonium hydroxide yielded amide **14**. Amide **14** maintained moderate p38α enzyme potency and improved

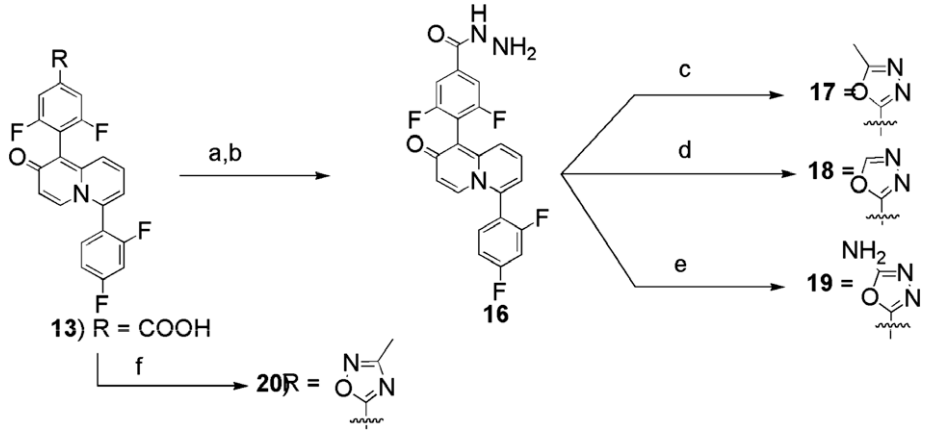

Scheme 2. Synthesis of 2,4,6 substituted A-ring 2*H*-quinolizin-2-one bioisostere derivatives. Reagents and conditions: (a) oxalyl chloride, DMF, DCM, 0 °C, quant.; (b) N_2H_4, CH_2Cl_2, rt, quant.; (c) trimethylorthoacetate, 120 °C, MeOH, 1.5 h; (d) triethylorthoformate, 110 °C, MeOH, 2 h, three step yield 6%; (e) cyanogen bromide, MeOH, 90 °C, 2 h, three step yield 9%; (f) EDC, hobt, *N*′-hydroxyethanimidamide, NMP, 90 °C, 6 h, 16%.

Table 3
Biological activity of 2,4,6 substituted A-ring 2*H*-quinolizin-2-one bioisostere derivatives

	p38α IC_{50} (nM)	THP-I/TNF-α[12] IC_{50} (nM)	hWB/TNF-α[6] IC_{50} (nM)	PXR EC_{50} (μM)
17	14	950	2660	>30
18	5.3	265	775	>30
19	6.8	270	1580	>30
20	8.8	430	690	>30

whole blood potency to sub micromolar levels. Methyl ester **15** possessed 1.5 nM p38α activity but failed to improve functional activity, therefore it was believed that metabolic stability of compounds **12**, **14**, and **15** were responsible for the large shift in functional activity. As a result, we explored suitable bioisostere replacements, such as oxadiazoles, for compounds **12**, **14**, and **15**.

Oxadiazole bioisosteres **17–20** were synthesized from carboxylic acid intermediate **13** (Scheme 2). Treatment of acid **13** with oxalyl chloride and catalytic amounts of DMF yielded the acid chloride derivative, which reacted with hydrazine hydrate to provide benzhydrazide **16**. The crude benzhydrazide intermediate was refluxed in trimethyl orthoacetate to yield oxadiazole **17** in low yield. Similarly, oxadiazoles **18** and **19** were synthesized from intermediate **16** using triethylorthoformate and cyanogen bromide, respectively. EDC/hobt amide coupling between **13** and *N*′-hydroxyethanimidamide and cyclization yielded oxadiazole **20** in a one pot reaction.

Oxadiazole bioisosteres **17–20** retained an excellent PXR profile (EC_{50} >30 μM) and improved WB and THP-1 potency relative to compounds **14** and **15**, but possessed functional activity several orders of magnitude weaker than lead compound **6** (Table 3). A-rings possessing a 4 substituted oxadiazole demonstrated that PXR activity can be successfully eliminated while retaining p38α enzyme potency, however other substitution patterns were explored to also increase functional activity. Previous manuscripts indicated an ortho substituted A-ring was critical for maintaining good enzyme potency.[15] Shifting the oxadiazole to the 5-position could exploit this group's PXR reducing properties and take advantage of the potency enhancing effects associated with a 2 fluoro group.

2,5 Substituted analogs **22** and **23** were synthesized by brominating 4-fluoro-3-methylbenzonitrile with *N*-bromosuccinimide and benzoyl peroxide to yield **21** (Scheme 3). Using a similar synthetic protocol as Schemes 1 and 2, bromide **21** was synthetically modified to yield derivatives **22–23**.

2,5 Substituted analogs possessed PXR activity and enzyme potency comparable to the 2,4,6 substituted series, while functional activity dramatically improved (Table 4). For example, THP-1 and WB activity of oxadiazoles **22** and **23** increased 10–30-fold and 15–60-fold, respectively when compared to 2,4,6 substituted analogs **17** and **18**. As with other 2*H*-quinolizin-2-one derivatives, compounds **22** and **23** possessed Ca and *i*Kr ion channel activity greater then 20 μM and 30 μM, respectively.

Pharmacokinetic properties of compounds **22** and **23** were evaluated in several species (Table 5). Compound **22** possessed good oral bioavailability, low clearance, and high AUC in all species tested. However, the half life of compound **22** in the dog IV study was still comparable to lead compound **6**. Compound **23** also possessed good oral bioavailability, low clearance, and high AUC, and a shorter half life in the dog pharmacokinetic studies. Therefore, compound **23** possessed the most desirable profile with potent functional activity, no ion channel or PXR off target activity, excellent kinase selectivity,[17] and a PK profile suitable for oral dosing in several species.

Efficacy was measured using the LPS induced arthritic rodent model to gauge the ability of **23** to decrease high levels of TNF-α

Table 5
Pharmacokinetic profiles of **22** and **23**

	Species	Cl (ml/min/kg)	AUC (μM h)	$T_{1/2}$ (h)	*F* (%)
22	Rat[a]	3.1	25.6	1.8	100
	Dog[b]	0.49	49.3	30.4	45
	Monkey[b]	3.6	5.1	5.9	47
23	Rat[a]	2.4	21.7	1.4	68
	Dog[b]	0.88	58.6	12.0	66
	Monkey[b]	0.90	23.9	9.5	55

[a] Iv 1 mg/kg, po 2 mg/kg, PEG-200/water 70:30 (v/v).
[b] Iv 0.25 mg/kg, ethanol/PEG-200/water (10:40:50) (v/v/v) po 2 mg/kg, 0.5% methylcellulose + 0.02% SDS.

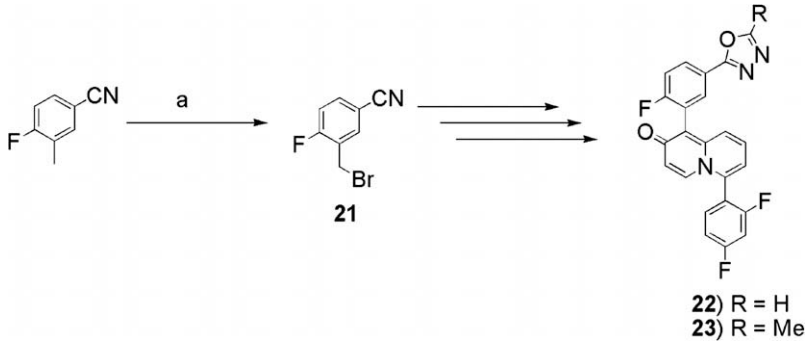

Scheme 3. Synthesis of 2,5 substituted A-ring 2*H*-quinolizin-2-one derivatives. Reagents: (a) NBS, benzoyl peroxide, CCl_4, reflux, 75%.

Table 4
Biological activity of 2,5 substituted A-ring 2*H*-quinolizin-2-one derivatives

	p38α IC_{50} (nM)	THP-I/TNF-α[12] IC_{50} (nM)	hWB/TNF-α [6] IC_{50} (nM)	PXR EC_{50} (nM)	Ca^{2+} IC_{50}[a] (μM)	*i*Kr[b] K_i (μM)
22	14.7	23.8	62.2	22.8	>30	>20
23	13.0	25.4	45.4	26.8	>30	>20

[a] Inhibition of diltiazem binding.[13]
[b] Inhibition of MK-499 binding to hERG in HEK293 cells.[14]

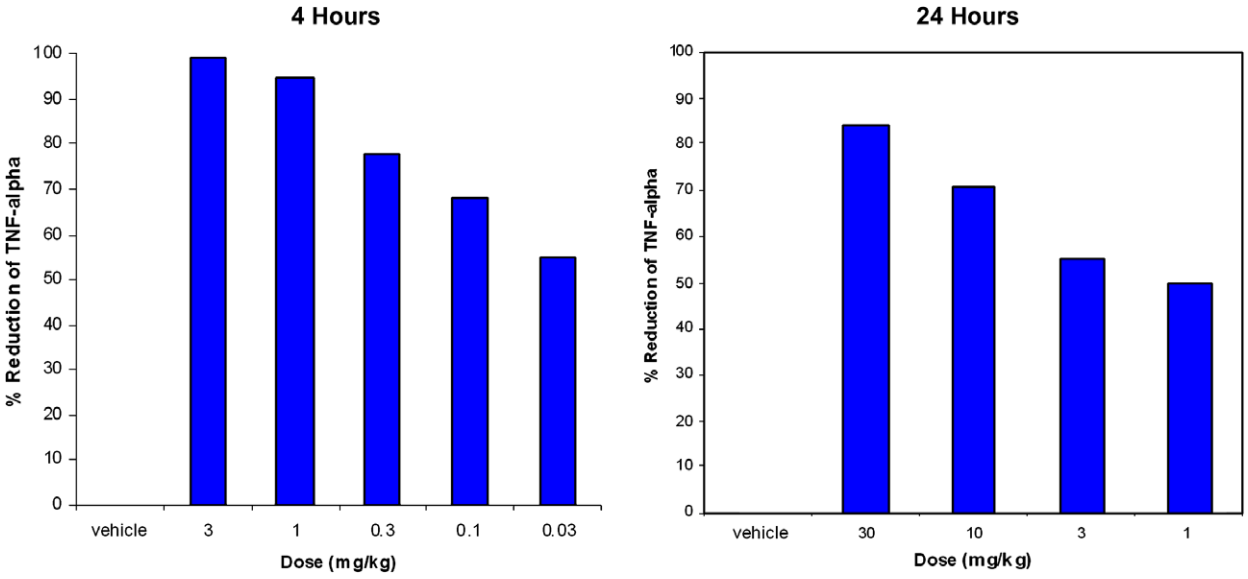

Figure 3. Reduction of TNF-α levels in rat LPS induced arthritic model at 4 and 24 h.

(Fig. 3). At the 4 h time point both 1 mg/kg and 3 mg/kg displayed >90% reduction of TNF-α levels, while 0.03 mg/kg still reduced THF-α levels by an average of 50%. The 24 h time point showed significant reduction in TNF-α levels at 30 and 10 mg/kg and moderate reduction at 1 and 3 mg/kg. Although the rat $t_{1/2}$ was 1.4 h, the excellent physical properties and potent functional activity of compound **23** allowed for excellent coverage in the 24 h LPS model.

In conclusion, we were able to successfully eliminate off target activity associated with piperazine **4** by removing the basic amine. Adjusting the core polarity to maintain functional potency led to the discovery of the novel 2*H*-quinolizin-2-one class of p38α inhibitors. Initially this series was plagued with high PXR activity and long half life, but SAR optimization of **6** solved such issues while maintaining excellent potency. Moreover, **23** proved efficacious in the LPS induced arthritic rat model.

References and notes

1. (a) Palladino, M. A.; Bahjat, F. R.; Theodorakis, E. A.; Moldawer, L. L. *Nat. Rev. Drug Disc.* **2003**, *2*, 736; (b) Saklatvala, J. *Curr. Opin. Pharmacol.* **2004**, *4*, 372.
2. Stoll, J. G.; Yasothan, U. *Nat. Rev. Drug Disc.* **2009**, *8*, 693.
3. Kobelt, G.; Eberhardt, K.; Geborek, P. *Ann. Rheum. Dis.* **2004**, *63*, 4.
4. Kumar, S.; Boehm, J.; Lee, J. C. *Nat. Rev. Drug Disc.* **2003**, *2*, 717.
5. (a) Lee, J. C.; Laydon, J. T.; McDonnell, P. C.; Gallagher, T. F.; Kumar, S.; Green, D.; McNulty, D.; Blumenthal, M. J.; Heys, J. R.; Landvatter, S. W.; Strickler, J. E.; McLaughlin, M. M.; Siemens, I. R.; Fisher, S. M.; Livi, G. P.; White, J. R.; Adams, J. L.; Young, P. R. *Nature* **1994**, *372*, 739; (b) Han, J.; Lee, J. D.; Bibbs, L.; Ulevitch, R. J. *Science* **1994**, *265*, 808.
6. Liverton, N. J.; Butcher, J. W.; Claiborne, C. F.; Claremon, D. A.; Libby, B. E.; Ngyuen, K. T.; Pitzenberger, S. M.; Selnick, H. G.; Smith, G. R.; Tebben, A.; Vacca, J. P.; Varga, S. L.; Agarwal, L.; Dancheck, K.; Forsyth, A. J.; Fletcher, D. S.; Frantz, B.; Hanlon, W. A.; Harper, C. F.; Hofsess, S. J.; Kostura, M.; Lin, J.; Luell, S.; O'Neil, E. A.; Orevillo, C. J.; Pang, M.; Parsons, J.; Rolando, A.; Sahly, Y.; Visco, D. M.; O'Keefe, S. J. *J. Med. Chem.* **1999**, *42*, 2180.
7. (a) Bemis, G. W.; Salituro, F. G.; Duffy, J. P.; Harrington, E. M. U.S. Patent 6147,080, 2000.; (b) Salituro, F.; Bemis, G.; Cochran, J. WO 99/64400.
8. (a) Natarajan, R. S.; Doherty, J. B. *Curr. Top. Med. Chem.* **2005**, *5*, 987; (b) Herberich, B.; Cao, G.-Q.; Chakrabarti, P. P.; Falsey, J. R.; Pettus, L.; Rzasa, R. M.; Reed, A. B.; Reichelt, A.; Sham, K.; Thaman, M.; Wurz, R. P.; Xu, S.; Zhang, D.; Hsieh, F.; Lee, M. R.; Syed, R.; Li, V.; Grosfeld, D.; Plant, M. H.; Henkle, B.; Sherman, L.; Middleton, S.; Wong, L. M.; Tasker, A. S. *J. Med. Chem.* **2008**, *51*, 6271.
9. Fitzgerald, C. E.; Patel, S. B.; Becker, J. W.; Cameron, P. M.; Zaller, D.; Pikounis, V. B.; O'Keefe, S. J.; Scapin, G. *Nat. Struct. Biol.* **2003**, *10*, 764.
10. Natarajan, S. R.; Heller, S. T.; Nam, K.; Singh, S. B.; Scapin, G.; Patel, S.; Thompson, J. E.; Fitzgerald, C. E.; O'Keefe, S. J. *Bioorg. Med. Chem. Lett.* **2006**, *16*, 5809.
11. A SPA-bead based assay was carried out using mouse p38. Compounds were serially diluted into a 96 well plate containing a MOPS based p38 assay buffer. The assay was initiated by addition of cold ATP, ^{33}P ATP (gamma) and biotin labeled GST-ATF2 substrate (4 μM). After incubation at 30 °C for 3 h, the reaction was stopped by addition of a PBS based quench buffer with 2× moles of SPA beads over the amount of substrate used. The extent of phosphorylation of GST-ATF2 was measured using a topcount reader and subtracted from background. IC_{50}s are means of two experiments.
12. Anti human TNF-α was coated on immulon four plates. THP-1 cells (density = 2.5×10^6/mL) were suspended into 96-well plates containing a PBS based medium. Compound was added as solution in DMSO followed by addition of LPS. The reaction was incubated for 4 h at 37 °C under CO_2. TNF-α release was measured in the supernatants by ELISA. Reported IC_{50}s are means from three measurements.
13. Ferry, D. R.; Glossman, H. *FEBS Lett.* **1982**, *148*, 331.
14. Butcher, J. W.; Claremon, D. A.; Connolly, T. M.; Dean, D. C.; Karczewski, J.; Koblan, K. S.; Kostura, M. J.; Liverton, N. J.; Melillo, D. G. WO 0205860, 2002.
15. Liu, L.; Stelmach, J. E.; Natarajan, S. R.; Chen, M. H.; Singh, S. B.; Schwartz, C. D.; Fitzgerald, C. E.; O'Keefe, S. J.; Zaller, D. M.; Schmatz, D. M.; Doherty, J. B. *Bioorg. Med. Chem. Lett.* **2003**, *13*, 3979.
16. Natarajan, S. R.; Chen, M.-H.; Heller, S. T.; Tynebor, R. M.; Crawford, E. M.; Minxiang, C.; Kaizheng, H.; Dong, J.; Hu, B.; Hao, W.; Chen, S.-H. *Tetrahedron Lett.* **2006**, *47*, 5063.
17. Upstate Biotechnology Inc. Kinase counterscreen against 180 kinases with no activity below 10 μM.